A BOX–BEHNKEN DESIGN-BASED MODEL FOR PREDICTING POWER PERFORMANCE IN MICROBIAL FUEL CELLS USING WASTEWATER

E.J. Martínez-Conesa, V. M. Ortiz-Martínez, M. J. Salar-García, A. P. De Los Ríos, F.J. Hernández-Fernández, L.J. Lozano, and C. Godínez

Although modelling is regarded as a useful tool to understand the performance of microbial fuel cells (MFCs), the number of MFC models remains very low compared with the number of experimental works available in the literature. Moreover, there are very few MFC modelling attempts dealing with the use of wastewater as fuel in these devices, which is essential for the practical implementation of MFCs since the potential of this technology lies in the two-fold benefit of wastewater treatment and bioenergy generation. In this work, a four-factor three-level Box–Behnken design was developed to model the electrochemical power generation in two-chamber MFCs using wastewater as fuel. The optimum values of temperature, external resistance, feed concentration and anodic pH that maximized power output were investigated. Optimum conditions were found at T = 35°C and R = 1kΩ, corresponding to a maximum power density of 0.88 $W \cdot m^{-3}$, while feed concentration and pH did not show statistical significance in the ranges studied. Thus, a Box–Behnken design-based model as empirical approach could provide an effective tool for the optimization study of MFC systems.

Keywords: Microbial fuel cells; Modelling; Optimization; Power density; Response surface methodology; Wastewater treatment.

Introduction

Microbial fuel cells (MFCs) are a promising technology dealing with two of the most pressing issues that modern society has to face such as demands for renewable non-fossil fuels and the needs for usable water (Cheng et al., 2014; Logan et al., 2006; Salar-García et al., 2015). In an MFC, bacteria degrade organic matter present in wastewater producing electrons and protons (Liu et al., 2004; Menicucci et al., 2006). If bacteria are properly attached to a conductive electrode material, electrons released as result of the oxidation

reaction at the anode can be transferred to the cathode through an external circuit (Duteanu et al., 2010; Guo et al., 2014; Ortiz-Martínez et al., 2015a). In order to balance the cell, protons go from the anode to the cathode through an internal membrane or separator. Electrons and protons are consumed at the cathode usually in an oxygen reduction reaction (ORR) to form water. Thus, there is an electromotive force in the cell due the half-reactions taking place at the cathode and anode electrodes (Deng et al.,2010; Hernández-Fernández et al., 2015; Yu et al., 2007).

The levels of power output generated in these devices are still relatively low and therefore research efforts are being concentrated on improving MFC performance (Degrenne et al., 2012; Kiely et al., 2011; Lanas et al., 2014; Wanget al., 2013). Modelling is a powerful tool for studying and optimizing the operation of MFCs because mathematical models can describe the processes that occur in these systems, covering multiple scenarios with significant savings in terms of cost and time. Although there has been a growing interest in MFC modelling in the last years with a resulting increase in the number of MFC models released, this type of work remains scarce in comparison with the number of experimental studies available (Oliveira et al., 2013). Among them, several computational models focusing on the anode as limiting factor have been reported given the importance of biofilm formation in MFCs (Ortiz-Martínez et al., 2015b). The model developed by Marcus et al. (2007) can be highlighted as one of the most prominent models belonging to this group. Their approach focuses on the electrical conduction properties of the biofilm formed in the anode chamber. This one-dimensional model employs the Monod and Nernst equations, anode-based mass balances and Ohm's law to describe the electrochemical performance of the system. Picioreanu et al. (2007) also presented a model based on the microbial activity of the anode, incorporating the Butler–Volmer expression to calculate the current density generated in an electrochemical mediator-based oxidation process. Picioreanu et al. (2008) integrated the before mentioned model with the IWA Model (ADM-1) (Batstoneet al., 2002) to cover the competition between anodophilic and methanogenic microbial communities, since methanogenesis phenomenon severely limits MFC efficiency. Pinto et al. (2010) reported a two-population model taking into account the competition between these two types of microbial communities.

On the other hand, there are a few models studying both the anode and the cathode compartments from an overall viewpoint, avoiding any a priori assumption that the anode is the limiting factor of the system. In this context, Zeng et al. (2010) used the Monod and Bulter–Volmer equations to describe the electrochemical performance of double-chamber MFCs. With a similar approach, Oliveira et al. (2013) followed the model proposed by Zeng et al. (2010) including the study of heat transport phenomena. Sirinutsomboon(2014) presented a comprehensive model for single-chamber MFCs in the absence of separator, comprising the modelling of biofilm formation by the Nernst–Monod equations and distinguishing between endogenous and exogenous respiration processes.

Finally, there are other works mainly focusing on the modelling of a key process or component, such as ionic transport through ion exchange membranes used as separator in MFCs (Harnisch et al., 2009) or the polarization response of these systems (Wen et al., 2009). Predictive techniques and mathematical algorithms have been also used in this field. Stratford et al. (2014) investigated the capability of several biological indexes in predicting MFC power performance, and Yan and Fan (2013) used fuzzy control combined with PID control to study double-chamber MFCs.

As can be seen above, several modelling approaches concerning MFCs have been developed. However, the majority of them employ pure substrates and synthetic wastewater prepared in the laboratory (e.g., acetate as carbon sourceand Shewanella putrefaciens as bacteria population). There are very few attempts to model MFCs using wastewater, despite the importance of this approach for the practical implementation of MFCs since the great potential of this technology lies in the twin advantage of treating wastewater and generating bioelectricity (Wen et al., 2009). These include the work by Alavijeh et al. (2015a), who proposed a one-dimensional model based on the spatial distributions of the different microorganisms including syntrophic interactions. They also combined several approaches from previous models in order to predict the performance of MFCs using simple and complex substrates such as dairy wastewater (Alavijeh et al., 2015b). Besides, to the best of our knowledge, there is no attempt in the open literature providing Box–Behnken-based empirical models to these devices. This empirical approach offers a useful substitute for pilot scale or scale-up optimization studies. Response surface design methodology (RSM) is based on a sequential set of designed

experiments to achieve the optimal response, allowing the relationships between controlled and response variables to be studied for the optimization of a given process. Box–Behnken designs are a well-known optimization tool that has been applied to many chemical processes (Chaichi et al., 2013; Ferreira et al., 2007; Li et al., 2010). This work presents a four-factor three-level Box–Behnken design to describe the electrochemical performance of an experimental two-chamber MFC, studying factors and operational parameters in MFC technology such as temperature, external resistance, feed concentration, and anodic pH that maximize power output.

Materials and Methods

Fuel and Reagents

Wastewater from the primary clarifier of a local wastewater treatment plant was used as organic matter source to inoculate the MFCs set up in the present work (Murcia-Este Plant, Spain). The wastewater used was characterized with a soluble chemical oxygen demand (COD) of 430 mg L^{-1}, total organic carbon (TOC) of 48.5 mg L^{-1}, volatile suspended solids (VSS) of 122% and suspended solids (SS) of 126 mg L^{-1}. The value of soluble COD was fixed at the desired level before each experiment by mixing raw wastewater with high COD wastewater from a local brewery industry (COD = 4100 mg L^{-1}). The final concentration was obtained by solving the set of equations in V_1 and V_2:

$$V_1 C_1 + V_2 C_2 = V_T C_T \quad (1)$$

$$V_1 + V_2 = V_T \quad (2)$$

where C_T is the desired COD in composite water, V_T is the desired volume in composite water, C_1, and C_2 are the known COD values for wastewater and brewery water, respectively, V_1, and V_2 are wastewater and brewery water volumes, respectively, and V_T is the desired volume in composite water.

Cathode compartments were filled with phosphate buffer solution, pH 7.0 (monobasic and dibasic potassium phosphates, Sigma-Aldrich, USA). The pH in the anode chamber was adjusted by adding dropwise solutions of acetic acid (for acidic set points) and sodium hydroxide (for basic set points) up to the desired value and monitoring the pH of

the mixture by using a pH meter. When COD and pH adjustments were both required, COD adjustment is performed in the first place followed by pH adjustment. These chemicals were purchased at the highest purity available (Sigma-Aldrich, Spain).

MFC Construction and Operation

The experimental MFC set-up consisted of double-chambered cells, each comprising two 250mL glass bottles to form the anode and the cathode chambers, respectively. Experiments were run in batch mode in cycles of 216 h in the absence of anode recirculation and stirring. The bottles were water-jacketed to keep the operating temperature constant (Schott, Germany). Both chambers were connected with a straight glass tube acting as a bridge (inner diameter of 1.5 cm). A proton exchange membrane Nafion-117 (DuPont Co., USA) acting as separator was placed between the anode and the cathode chambers by using rubber gaskets and 30mm rounded metal joint clips (J.P Selecta, Spain). The temperature of the reactors was controlled with a circulation bath Frigiterm-10 (J.P Selecta, Spain) (minimum cooling temperature of 10°C and a maximum heating temperature of 100°C). An aquarium aerator and porous diffusers were used to supply oxygen to the cathode chamber. Figure 1 shows a schematic representation of the MFC system used for the present work.

The anode electrodes were made of carbon cloth (E-TEK, USA) while the cathodes consisted of platinized titanium (William Gregor Ltd., UK), both prepared with the same dimensions of 3x2 cm^2. Nafion-based membranes were pre-treated in oxygen peroxide (30% H_2O_2) and deionized water at 80°C for one hour, respectively, followed by 0.5M H2SO4 at 80°C for a further hour. Both electrodes and membranes were kept in deionized water before each use. Electrodes were connected with titanium wires of 30 cm in length (Sigma-Aldrich, USA). In experiments requiring resistance load, anodes and cathodes were connected in closed circuit with an external resistance load of 1 kΩ.

A central hole was drilled on the anode chamber cap to house the electrode. Oxygen was removed from anode chamber by bubbling nitrogen during the start-up of the MFCs investigated through the anode. Nut-and-septum inserts and polypropylene tubing were used for anode sampling to avoid the exposure of the anode chamber to the open air.

Anode chambers were covered with aluminium foil to avoid typical light and temperature day-night cycles.

Analytical Methods and Measurements

Organic soluble matter concentration was measured as COD (mg L^{-1}), which is defined as the amount of oxygen necessary to completely oxidize the organic matter contained in a sample. COD measurements were carried out by using the method described in APHA et al. (2005). Anode sampling was conducted on a daily basis. 3 mL of sample were 0.45 mm filtered (Millipore, Spain) and then added to a test tube containing enough amounts of COD reagents (Merck, Germany), with a final sample concentration in the 25–1500 mg L^{-1} range. Samples were digested during two hours at 150°C in an ECO16 thermoreactor (Velp Scientifica, Italy) until reaction was complete. COD was measured in a Spectroquant NOVA 30 (Merck, Germany). The percentage of elimination of soluble organic matter (% COD) is expressed as a percentage with respect to the initial COD. pH measurements were monitored with a pH electrode (Crison Cat. N. 52-04) connected to a pH and conductivity measurement device with temperature compensation (Crison micropH 2000). The accuracy of the measurement was ±0.01 pH units.

Voltage was measured by using a DVM-891 digital polymeter (HQ Power, Germany) clipped to both sides of the external resistance load. Current (I) was calculated from Ohm's law:

$$I = \frac{E_{cell}}{R_{ext}} \quad (3)$$

where E_{cell} is the potential of the cell and R_{ext} is the external resistance load.

Thus, power (P) can be calculated as:

$$P = \frac{E_{cell}^2}{R_{ext}} \quad (4)$$

power is usually normalized to one of the characteristics of the MFC reactors. This way, power outputs from different systems can be compared. In this work, power output was normalized to the volume of the reactor. This allows engineering calculations for size and costing of reactors to be performed:

$$P_V = \frac{E_{cell}^2}{VR_{ext}} \quad (5)$$

where P_v is the power density (Wm^{-3}) and V is the total reactor volume (empty bed volume).

Results and Discussion

Box–Behnken Design-Based Model

The experimental design was selected according to a Box–Behnken matrix (see Supporting Information) with high and low levels determined by the maximum and minimum of the experimental range for each variable, respectively. Temperatures in the experimental space ranged from 15°C to 35°C, wastewater feed concentration from 500 to 1500 mg L^{-1}, external resistance from 1 to 100 kΩ and pH from 5 to 9 units. Having these four factors to be investigated, the number of possible scenarios are 28, including 4 replicates in order to assess experimental error (experimental numbers 11, 14, 26 and 28 in Table I). Experiments were executed in blocks of 8 experiments and in a random order between blocks so that any possible bias from previous results was avoided. The experimental operation of fed-batch MFCs in closed circuit goes through several stages. After an induction phase for the accommodation of microorganisms, there is an exponential growth followed by a stationary phase and a final declining phase. The duration of each phase depends on the initial content of organic matter and the type of oxidant. Examples of the experimental results are depicted in Figures 2 and 3, in which power density and COD removal evolution are plotted as a function of time for some selected experiments. Response used for the model was maximum power density, which typically develops after 24–72 hours depending on the experimental conditions. In this model, the levels of four variables, temperature (T), external resistance (R), wastewater

initial concentration (C) and anodic pH was investigated for the maximization of power density. A summary with all experimental results is shown in Table I, which includes the maximum power obtained for the conditions established in each scenario. According to the RSM method, a quadratic model where ε is the experimental error will suit for the purpose (Equation (4)):

$$y = \beta_0 + \sum_{i=1}^{k} \beta_i x_i + \sum_{i=1}^{k} \beta_{ii} x_i^2 + \sum_{j=2}^{k} \sum_{i=1}^{j-1} \beta_{ij} x_i x_j + \varepsilon \quad (6)$$

This empirical model approach is very useful since it is easy to estimate and apply, especially when little is known about the process. Equation (6) can be rewritten in the matrix form for our particular case:

$$[P_V] = [X][\beta] \quad (7)$$

where matrix [X] represents the independent terms (namely, temperature, external resistance, wastewater concentration and pH), matrix [P_V] is the volumetric power density (W m^{-3}), and matrix [β] is the matrix of the coefficients of the model. As [X] is not a square matrix (and consequently it lacks inverse), transposition of matrix X is needed in order to solve the equation in [β]:

$$[\beta] = \left[[X^T][X]\right]^{-1}[X][P_V] \quad (8)$$

Model Resolution

In this paper, several forms of Equation (6) were solved with the aid of commercial software Sagata. These forms were linear, linear+interactions, quadratic (without interactions) and full quadratic (including interactions). An ANOVA analysis was performed in all cases and regression coefficient (r^2), residual sum of squares (RSS), and lack-of-fit (p-value) were registered and are summarized in Table II and in detail only for the full quadratic model in Table III. As can be seen from Table II, the values of r^2 increases and the residual sum of squares (S) reduces as number of parameters in the model rises. Only quadratic and full quadratic models showed a significant correlation

(p-value for lack-of-fit > 0.05). However, even with those models regression coefficients, r^2 values were relatively low (around90%). The four replicates conducted (experiments numbers 11, 14, 26, and 28) ranged from a power density from 0.029 to 0.179 Wm^{-3} with a mean of 0.102 Wm^{-3} and a standard deviation of 0.057 Wm^{-3}. This limited repeatability is recognized in the literature (Larrosa et al., 2009) and is responsible for the relatively low r^2 and RSS values found with ANOVA.

A plot of the main effects for the linear model is represented in Figure 4. These plots can be used to compare the magnitudes of the various main effects. A main effect occurs when the mean response changes across the levels of a factor (the red dotted line is the grand mean of the response data). Therefore, the main effect plots can be used to compare the relative strength of the factors. On the other hand, as can be observed in Figure 4, both initial wastewater concentration and pH were not statistically relevant (within the experimental space) for predicting power density as compared to temperature and external resistance. Also although the full quadratic model showed a polished correlation, these parameters showed to be non-significant (p-values > 0.05, 95%confidence). Therefore, in a further refinement they were removed. Finally, the best model for predicting power density was as follows:

$$P_V\left(\frac{W}{m^3}\right) = 0.09117 + 0.02257 \cdot T - 0.35942 \cdot logR + 0.21827(logR)^2 - 0.01593 \cdot T \cdot logR \quad (9)$$

where T represents the cell temperature, log (R) is the common logarithm of the external resistance, C is the wastewater initial concentration, and P is the pH of the contaminated fluid. The ANOVA for this model (see Table IV) shows an acceptable r^2 value balanced with a close to minimal RSS and all its parameters are statistically significant (p-values < 0.05, 95% confidence).

A view of the response surface is illustrated as a contour plot in Figure 5(a) and in a three-dimensional space in Figure 5(b). As can be observed, power density increases with temperature while it decreases as logR increases, which would indicate that the response of the system would be favoured by high and low values of temperature and external resistance load, respectively, within the ranges studied. Also, Figure 6 depicts the predicted values vs. observed values. These are scattered randomly along the diagonal

not following any pattern, which is in agreement with homoscedasticity hypothesis, in which these designs are based. Normality hypothesis of the data is also guaranteed as can be inferred from the plot of the quartiles of the normal distribution vs. the residuals (Figure 7). Once the prediction equation was shown to be sufficiently strong, it was used to obtain the conditions that maximize power density for the experimental MFCs. In order to make this optimization, partial derivatives of Equation (7) were taken with respect to each one to the factors and were equated to zero:

$$\frac{\partial P}{\partial T} = 0.02257 - 0.01593 logR = 0$$

$$\frac{\partial P}{\partial logR} = -0.35942 + 0.43654 logR - 0.01593 T = 0 \qquad (10)$$

The resulting set of two equations was subjected to constrained optimization by using Sagatac. The search was forced into the experimental space in order to avoid finding of unrealistic optimum values. Accordingly, operating conditions that yield maximum power density within the experimental design were found to be T = 35°C and R = 1 kΩ. Initial COD concentration and pH do not significantly affect the power within the experimental space studied. Under these conditions, the maximum power density was found to be 0.83Wm^{-3}. The trends marked in this study point out towards optimal performance for the MFC systems studied at high temperatures (i.e., hot climates) and external resistances relatively low within the interval analyzed (microelectronics). On the other hand, COD elimination was higher than 80% in all cases, showing its potential use in wastewater treatment. Finally, initial wastewater concentration within 500–1500 mg/L did not reveal statistical significance on power response and could be considered adequate for the MFC systems investigated. Other works that have studied this parameter in a wider range have reported that feed concentration must be balanced, since high organic load can favour the growth of methanogenic bacteria instead of anodophilic microbial populations. Methanogenic bacteria promote the production of CH_4 in the anode instead of boosting electrical performance, thus affecting the power output obtained (Pinto et al., 2010). In the same way, the effect of pH within the interval 5–9 on power performance was not significant, even when subjected to slightly acid pH conditions (pH = 5). Compared with other modelling approaches commented in the introduction part, Box–Behnken design-based models can present some limitations such as the lack of understanding of the

dynamic behaviour of the system. However, it can be especially useful when little is known about the process (Ferreira et al., 2007). Moreover, the optimum values could be used as starting point for searching optimum values with more sophisticated non-linear models.

Conclusions.

In this work, a four-factor three-level Box–Behnken design was built to predict the electrochemical power generation in two-chamber MFC systems using wastewater as fuel. Optimal values for temperature (T), external resistance (R), wastewater initial concentration (C), and anodic pH were investigated using a quadratic model including linear, linear+interactions, quadratic (without interactions) and full quadratic (including interactions) forms. Operating conditions that yield maximum power density within the experimental design were found to be T = 35°C and R = 1kΩ, while initial COD concentration and pH did not significantly affect the power within the experimental range tested. More MFC models are expected to be developed in the future due to their great advantages for off-line process optimization, especially models dealing with wastewater for the practical application of MFC technology for simultaneous production of energy and water treatment.

Aknowledgments.

This work has been supported by the Ministry of Science and Innovation of Spain (MICINN), ref. CICYT ENE2011-25188, and the Séneca Foundation Ref. 18975-JLI-13. V.M. Ortiz-Martínez and M.J. Salar-García are supported by grants FPU2012-05444 and BES-2012- 055350, respectively.

361 References

362

363 Alavijeh, M. K., Yaghmaei, S., and Mardanpour, M. M. (2015a). A combined model for
364 large scale batch culture MFC-digester with various wastewaters through different
365 populations, Bioelectrochem,106, 298–307.

366

367 Alavijeh, M. K., Mardanpour, M. M., and Yaghmaei, S. (2015b). One-dimensional
368 conduction-based modelling of bioenergy production in a microbial fuel cell engaged
369 with multi-population biocatalysts, Electrochem. Acta, 184, 151–163.

370

371 APHA, AWWA, WPFC. (2005). Standard Methods for Examination of Water and
372 Wastewater, 21th edition, American Public Health Association, Washington, DC.

373

374 Batstone, D. J., Keller, J., Angelidaki, I., Kalyuzhnyi, S. V.,Pavlostathis, S. G., Rozzi, A.,
375 Sanders, W. T. M., Siegrist, H.,and Vavilin, V. A. (2002). The IWA anaerobic digestion
376 model No 1 (ADM1), Water Sci. Technol., 45, 65–73.

377

378 Chaichi, M. J., Azizia, S. N., Alijanpoura, O., Heidarpoura, M., and Qandaleeb, M.
379 (2013). Application of Box–Behnken design in the optimization of new peroxyoxalate
380 H2O2 chemiluminescence system using furan derivatives as blue activators, J. Lumin.,
381 138, 65–71.

382

383 Cheng, S., Ye, Y., Ding, W., and Pan, B. (2014). Enhancing power generation of scale-
384 up microbial fuel cells by optimizing the leading-out terminal of anode, J. Power Sources,
385 248, 931–938.

386

387 Degrenne, N., Buret, F., Allard, B., and Bevilacqua, P. (2012). Electrical energy
388 generation from a large number of microbial fuel cells operating at maximum power point
389 electrical load, J. Power Sources, 205, 188–193.

390

391 Deng, Q., Li, X., Zuo, J., Ling, A., and Logan, B. E. (2010). Power generation using an
392 activated carbon fiber felt cathode in an upflow microbial fuel cell, J. Power Sources,
393 195, 1130–1135.

394

Duteanu, N., Erable, B., Kumar, S. M. S., Ghangrekar, M. M., and Scott, K. (2010). Effect of chemically modified Vulcan XC-72R on the performance of air-breathing cathode in a single-chamber microbial fuel cell, Bioresour. Technol., 101, 5250–5255.

Ferreira, L. C., Bruns, R. E., Ferreira, H. S., Matos, G. D., David, J.M., Brandao, G. C., da Silva, E. G. P., Portugal, L. A., dos Reis, P.S., Souza, A. S., and dos Santos, W. N. L. (2007). Box-Behnken design: An alternative for the optimization of analytical methods. Anal. Chim. Acta, 597, 179–186.

Guo, X., Zhan, Y., Chen, C., Zhao, L., and Guo, S. (2014). The influence of microbial synergistic and antagonistic effects on the performance of refinery wastewater microbial fuel cells, J. Power Sources, 251, 229–236.

Harnisch, F., Warmbier, R., Schneider, R., and Schröder, U. (2009). Modeling the ion transfer and polarization of ion exchange membranes in bioelectrochemical systems, Bioelectrochem, 75, 136–141.

Hernández-Fernández, F. J., Pérez de los Ríos, A., Salar-García, M. J., Ortiz-Martínez, V. M., Lozano-Blanco, L. J., Godínez, C., Tomás-Alonso, F., and Quesada-Medina, J. (2015). Recent progress and perspectives in microbial fuel cells for bioenergy generation and wastewater treatment, Fuel Process. Technol., 138, 284–297.

Kiely, P. D., Cusick, R., Call, D. F., Selembo, P. A., Regan, J. M., and Logan, B. E. (2011). Anode microbial communities produced by changing from microbial fuel cell to microbial electrolysis cell operation using two different wastewaters. Bioresour. Technol.,102, 388–394.

Lanas, V., Ahn, Y., and Logan, B. E. (2014). Effects of carbon brush anode size and loading on microbial fuel cell performance in batch and continuous mode, J. Power Sources, 247, 228–234.

Larrosa, A., Lozano, L. J., Katuri, K. P., Head, I., Scott, K., and Godínez, C. (2009). On the repeatability and reproducibility of experimental two-chambered microbial fuel cells. Fuel, 88, 1852–1857.

Li, M., Feng, C., Zhang, Z., Chen, R., Xue, Q., Gao, C., and Sugiura, N. (2010). Optimization of process parameters for electrochemical nitrate removal using Box–Behnken design, Electrochim. Acta,56, 265–270.

Liu, H., Ramanarayanan, R., and Logan, B. E. (2004). Production of electricity during wastewater treatment using a single chamber microbial fuel cell, Environ Sci. Technol., 38, 2281–2285.

Logan, B. E., Hamelers, B., Rozendal, R., Schro¨der, U., Keller, J.,Freguia, S., Aelterman, P., Verstraete, W., and Rabaey, K. (2006).Microbial fuel cells: Methodology and technology, Environ. Sci. Technol., 40, 5181–5192.

Marcus, A. K., Torres, C. I., and Rittmann, B. E. (2007). Conduction-based modelling of the biofilm anode of a microbial fuelcell. Biotechnol. Bioeng., 98, 1171–1182.

Menicucci, J., Beyenal, H., Marsili, E., Veluchamy, R. A., Demir, G., and Lewandowski, Z. (2006). Procedure for determining maximum sustainable power generated by microbial fuel cells, Environ. Sci. Technol., 40, 1062–1068.

Oliveira, V. B., Simo˜es, M., Melo, L. F., and Pinto, A. M. F. R. (2013). A1D mathematicalmodel for a microbial fuel cell, Energy, 61, 463–471.

Ortiz-Martínez, V. M., Salar-García, M. J., de los Ríos, A. P., Hernández-Fernández, F. J., Egea, J.A., and Lozano, L. J. (2015a). Developments in microbial fuel cell modeling, Chem. Eng. J., 271, 50–60.

Ortiz-Martínez, V. M., Salar-García, M. J., Hernández-Fernández, F. J. and de los Ríos, A. P., (2015b). Development and characterization of a new embedded ionic liquid based membrane-cathode assembly for its application in single chamber microbial fuel cells, Energy, 93,1748–1757.

Picioreanu, C., Head, I. M., Katuri, K. P., Loosdrecht, M. C. M., and Scott, K. (2007). A computational model for biofilm-based microbial fuel cells, Water Res., 41, 2921–2940.

Picioreanu, C., Katuri, K. P., Head, I. M., Loosdrecht, M. C. M., and Scott, K. (2008). Mathematical model for microbial fuel cells with anode biofilms and anaerobic digestion, Water Sci. Technol., 57,965–971.

Pinto, R. P., Srinivasan, B., Manuel, M.-F., and Tartakovsky, B.(2010). A two-population bio-electrochemical model of a microbialfuel cell, Bioresour. Technol., 101, 5256–5265.

Salar-García, M. J., Ortiz-Martínez, V. M., Hernández-Fernández, F.J., and de los Ríos, A. P. (2015). Scaled-up continuous up-flow microbial fuel cell based on novel embedded ionic liquid-type membrane-cathode assembly, Energy, 101, 113–120.

Sirinutsomboon, B. (2014). Modelling of a membraneless single-chamber microbial fuel cell with molasses as an energy source, Int. J. Energy Environ. Eng., 5, 1–9.

Stratford, J. P., Beecroft, N. J., Slade, R. T. C., Grüning, A., and Avignone-Rossa, C. (2014). Anode microbial community diversity as a predictor of the power output of microbial fuel cells, Bioresour. Technol., 156, 84–91.

Wang, X., Gao, N., Zhou, Q., Dong, H., Yu, H., and Feng, Y. (2013). Acidic and alkaline pretreatments of activated carbon and their effects on the performance of air-cathodes in microbial fuel cells, Bioresour. Technol., 144(2013), 632–636.

Wen, Q., Wu, Y., Cao, D., Zhao, L., and Sun, Q. (2009). Electricity generation and modelling of microbial fuel cell from continuous beer brewery wastewater, Bioresour. Technol., 100,4171–4175.

Yan, M., and Fan, L. (2013). Constant voltage output in two-chamber microbial fuel cell under fuzzy PID control, Int. J. Electrochem. Sci.,8, 3321–3332.

Yu, E. H., Cheng, S. A., Scott, K., and Logan, B. E. (2007). Microbial fuel cell performance with non-Pt cathode catalysts, J. Power Sources, 171, 275–281.

496 Zeng, Y., Choo, Y. F., Kim, B.-H., and Wu, P. (2010). Modelling and simulation of two-
497 chamber microbial fuel cell, J. Power Sources,195, 79–89.104
498

Table 1. Summary table with all experimental results

Test	T (°C)	log R	C (mg L^{-1})	pH	$P_{V,max}$ (*) (W m^{-3})	I_{max} (A m^{-2})
1	25	1	500	9	0.111	$3.002 \cdot 10^{-5}$
2	25	1	1500	9	0.172	$3.739 \cdot 10^{-5}$
3	35	1	1500	7	0.056	$2.141 \cdot 10^{-5}$
4	35	1	1000	9	0.091	$2.727 \cdot 10^{-5}$
5	35	2	1000	7	0.015	$3.539 \cdot 10^{-6}$
6	25	2	1500	7	0.018	$4.752 \cdot 10^{-6}$
7	15	1	500	7	0.056	$2.141 \cdot 10^{-5}$
8	15	0	1000	7	0.241	$1.406 \cdot 10^{-4}$
9	25	1	500	5	0.327	$5.179 \cdot 10^{-5}$
10	35	1	500	7	0.178	$3.795 \cdot 10^{-5}$
11	25	1	1000	7	0.029	$1.531 \cdot 10^{-5}$
12	15	1	1000	9	0.019	$1.239 \cdot 10^{-5}$
13	15	1	1500	7	0.009	$8.315 \cdot 10^{-6}$
14	25	1	1000	7	0.070	$2.352 \cdot 10^{-5}$
15	15	1	1000	5	0.217	$4.221 \cdot 10^{-5}$
16	25	2	500	7	0.024	$4.435 \cdot 10^{-6}$
17	15	2	1000	7	0.012	$3.094 \cdot 10^{-6}$
11	25	0	1000	9	0.848	$2.474 \cdot 10^{-4}$
19	35	0	1000	7	0.881	$1.628 \cdot 10^{-4}$
20	25	2	1000	9	0.006	$2.294 \cdot 10^{-6}$
21	25	1	1500	5	0.082	$2.598 \cdot 10^{-5}$
22	25	0	500	7	0.641	$2.293 \cdot 10^{-4}$
23	25	0	1000	5	0.713	$2.396 \cdot 10^{-4}$
24	25	0	1500	7	0.508	$2.012 \cdot 10^{-4}$
25	25	2	1000	5	0.005	$1.912 \cdot 10^{-6}$
26	25	1	1000	7	0.131	$3.301 \cdot 10^{-5}$
27	35	1	1000	5	0.130	$3.276 \cdot 10^{-5}$
28	25	1	1000	7	0.179	$3.817 \cdot 10^{-5}$

(*) Conversion from W m^{-3} to W m^{-2} may be accounted by multiplying volumetric power density by a $1.1 \cdot 10^{-4}$ factor which includes anode specific surface, anodic chamber surface-to-volume ratio and graphite density.

Table 2. Basic statistics of the model studied

Model	r^2(%)	S	Lack-of-fit (p-value)
Linear	61.5	0.1638	0.068
Linear + interactions	66.6	0.1790	0.040
Linear + quadratic	84.2	0.1165	0.0165
Full quadratic	90.1	0.1127	0.0163

Table 3. a) Regression and b) ANOVA data for the full quadratic model

a) Regression

Term	Coef.	SE Coef.	T	P
Constant	0.1022	0.05637	1.814	0.095
T	0.0565	0.03565	1.584	0.139
Log R	-0.3111	0.03565	-8.725	0.000
C	-0.0410	0.03255	-1.260	0.232
pH	-0.0106	0.03255	-0.325	0.751
T*T	-0.0504	0.04827	-1.045	0.317
Log R*Log R	0.2129	0.04827	4.411	0.001
C*C	-0.0009	0.04660	-0.019	0.985
pH*pH	0.0790	0.04660	1.695	0.116
T*logR	-0.1294	0.07130	-1.815	0.095
T*C	-0.0187	0.05637	-0.333	0.745
T*Ph	0.0397	0.05637	0.705	0.494
LogR*C	0.0317	0.05637	0.563	0.584
LogR*pH	-0.0585	0.05637	-1.038	0.320
C*pH	0.0765	0.05637	1.357	0.200
S = 0.1127	r^2 = 90.1%			

b) ANOVA

Source	DF	Seq SS	Adj SS	Adj MS	F	P
Regression	14	138.259	138.259	0.098756	7.77	0.001
Linear	4	0.94458	0.98931	0.247327	19.46	0.000
Square	4	0.34727	0.36040	0.090100	7.09	0.004
Interaction	6	0.09073	0.09073	0.015122	1.19	0.374
Lack-of-fit	9	0.13940	0.13940	0.015489	3.54	0.163
Pure error	3	0.01312	0.01312	0.004374		
Total	26	153.511				

Table 4. a) Regression and b) ANOVA data for the definitive model

a) Regression

Term	Coefficients	SE Coef.	T	P
Constant	0.1161	0.02846	4.079	0.000
T	0.0664	0.03549	1.871	0.045
Log R	-0.3210	0.03549	-9.045	0.000
LogR*LogR	0.2183	0.04549	4.798	0.000
T*LogR	-0.1593	0.06970	-2.285	0.032
S = 0.1138	R^2 = 85.4%			

b) ANOVA

Source	Degrees of freedom	Seq SS	Adj SS	Adj MS
Regression	4	125.009	125.009	0.31252
Linear	2	0.92307	106.429	0.53214
Square	1	0.25940	0.29828	0.29828
Interaction	1	0.06763	0.06763	0.06763
Lack-of-fit	3	0.08753	0.08753	0.02918
Pure error	19	0.19479	0.19749	0.01039
Total	26	153.511		

Figure 1. Schematic representation of the MFC system used

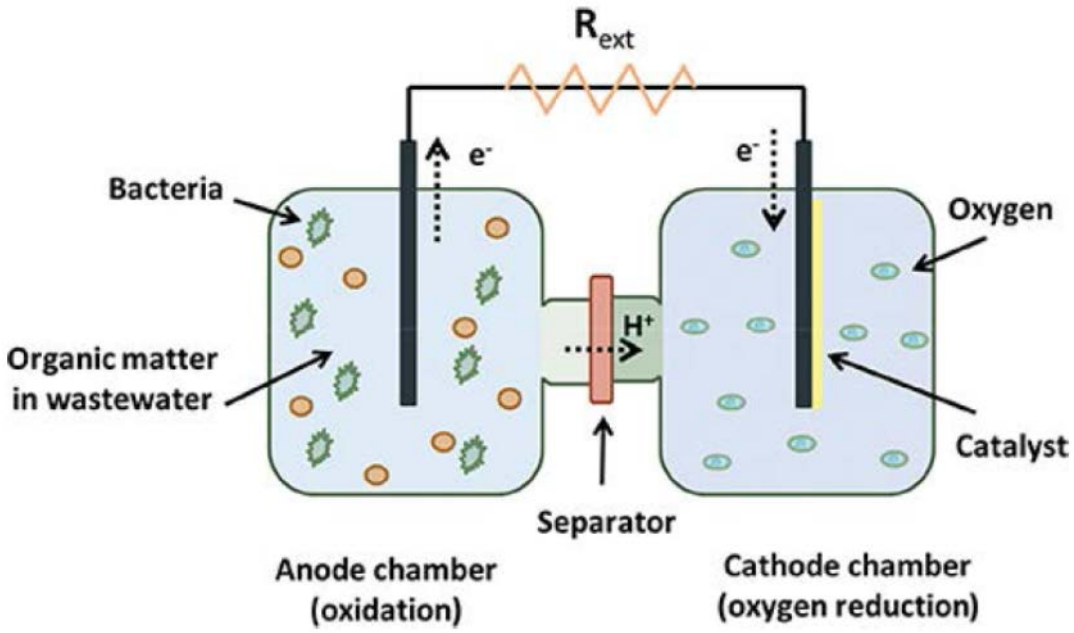

Figure 2. Volumetric power density as a function of time for some selected experiments

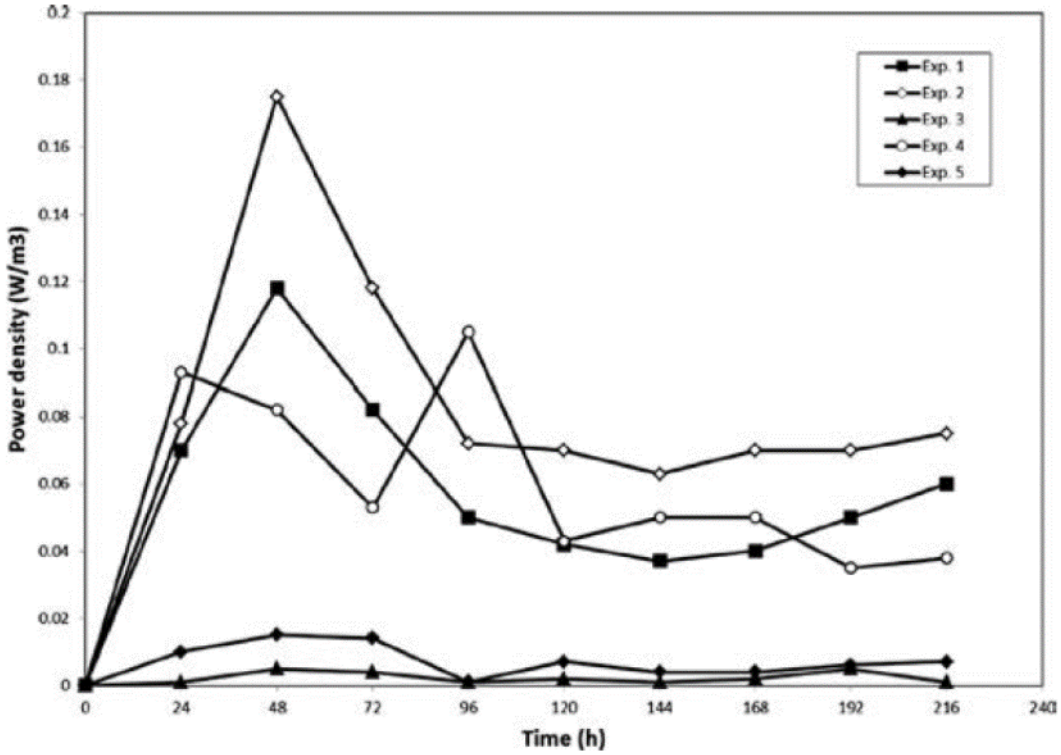

Figure 3. COD evolution as a function of time for some selected experiments.

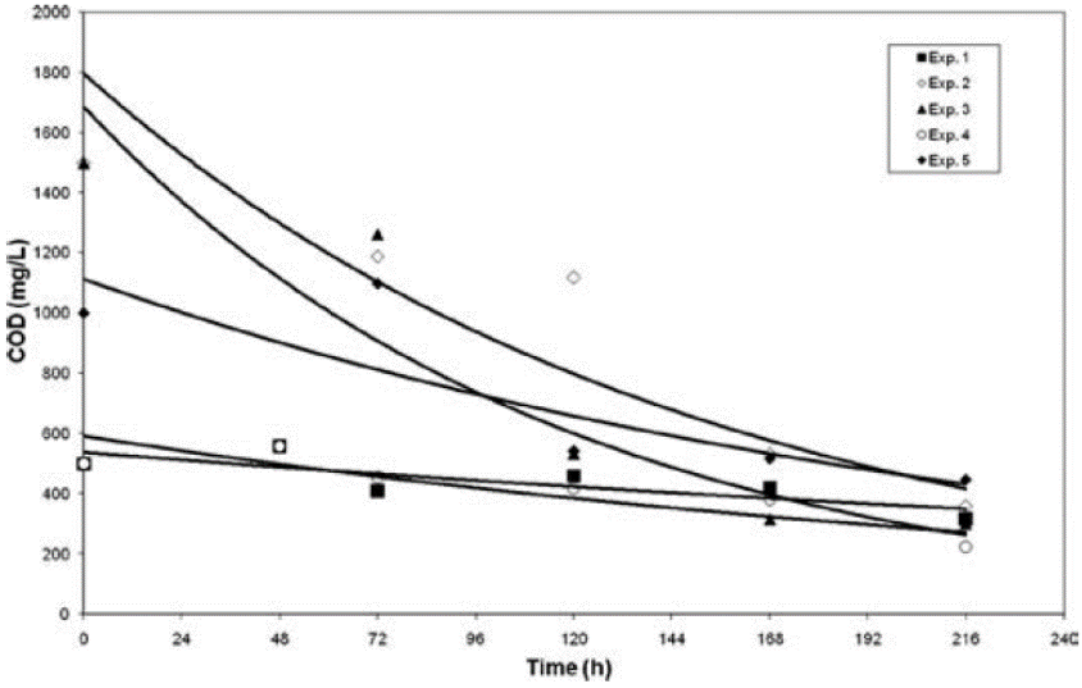

Figure 4. Main effects plots for the linear model.

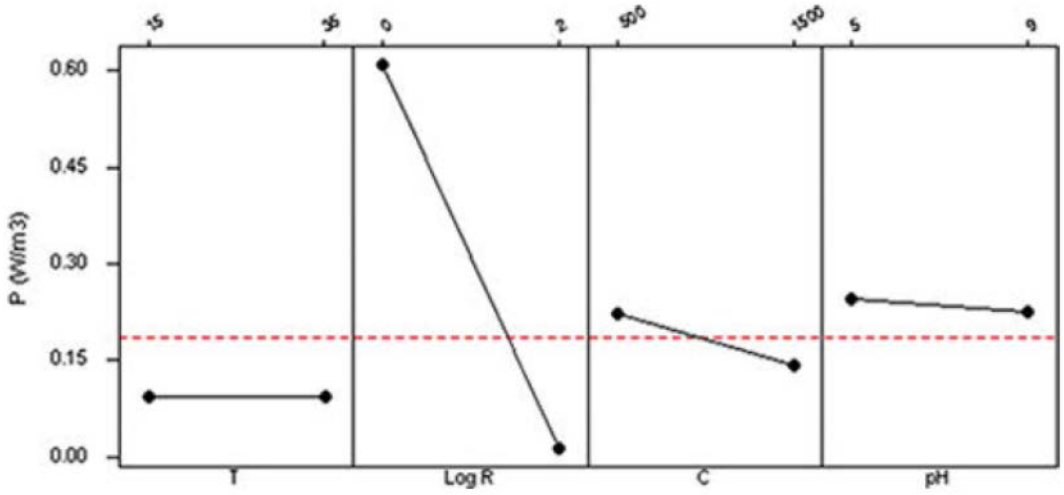

Figure 5. Graphical representation of the response surface as a function of T and R: a) Contour plot; b) Wireframe plot

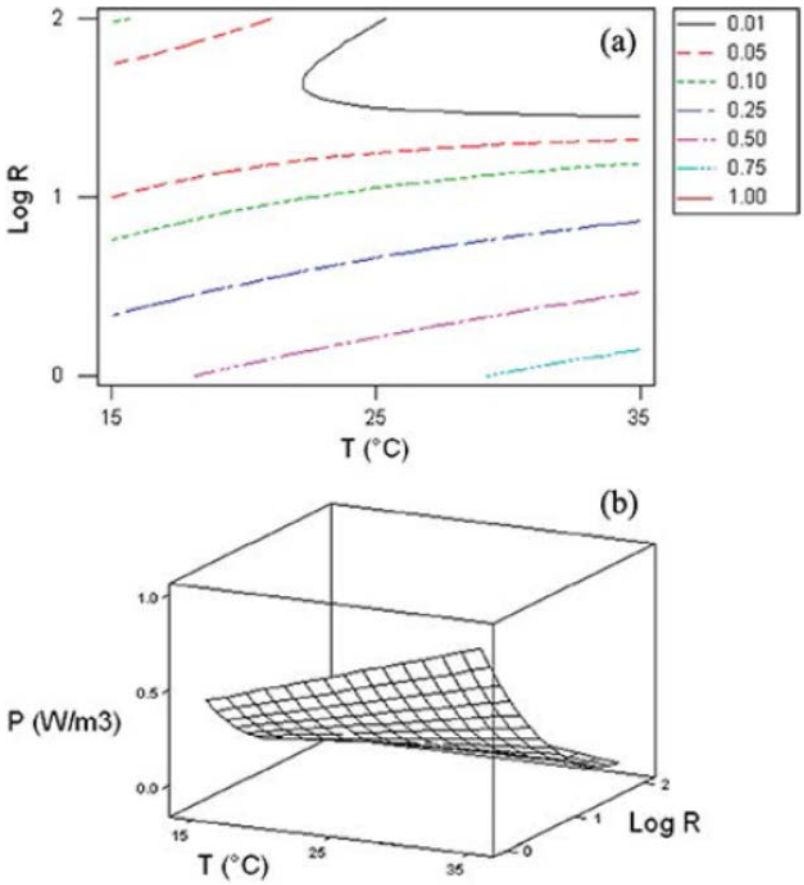

Figure 6. Model prediction vs observed values.

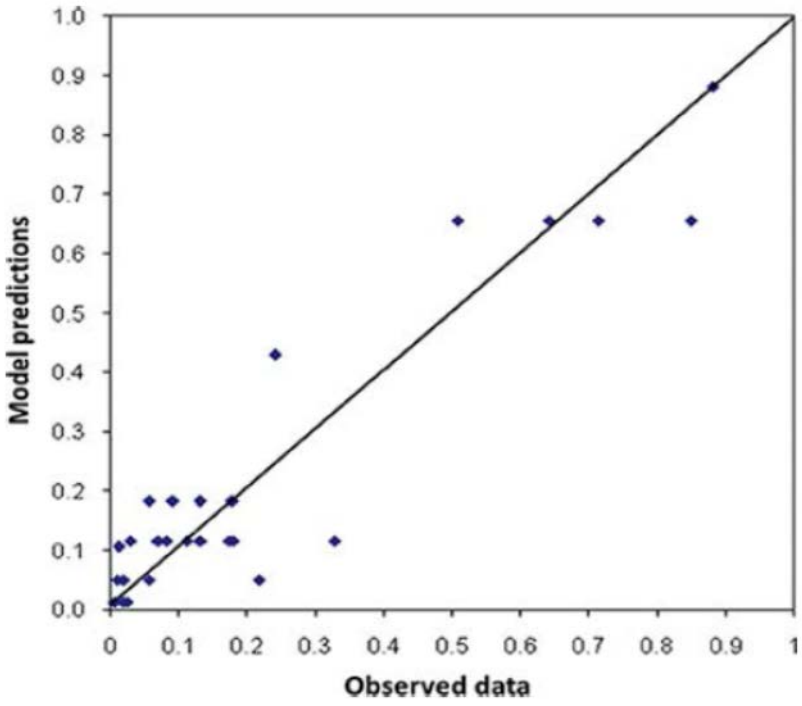

Figure 7. Normality test